7.3 A CODE FOR AUTOMATED DERIVATION OF POST NECKING TRUE STRESS-TRUE STRAIN CONSTITUTIVE LAWS FROM STANDARD TENSILE TEST ENGINEERING STRESS STRAIN CURVES —

Shuangyu Li, Takuya Yamamoto, G. Robert Odette (UCSB)

OBJECTIVES

Objectives of this study are to automate derivation of true stress-true stain constitutive [$\sigma(\varepsilon)$] beyond the strain range (necking) that standard uniaxial tensile tests can normally provide, especially in irradiated alloys that almost immediately neck.

SUMMARY

We previously developed a self-consistent approach to derive true stress-stain constitutive [$\sigma(\varepsilon)$] laws from measured tensile test engineering stress-strain $s(e)_m$ data based on finite element method (FEM) simulations. The simulated $s(e)_s$ were based on trial input $\sigma(\varepsilon)_n$ that were adjusted in an iterative fashion until convergence at $s(e)_s \approx s(e)_m$. The adjustments between $\sigma(\varepsilon)_n$ and $\sigma(\varepsilon)_{n+1}$ were based on experience and judgment but in some cases convergence required many time consuming iterations. Here we report an automated iterative process that is much more efficient and less time consuming for the researcher.

PROGRESS AND STATUS

Introduction

Deformation controlled failure of a structure is mediated by the interaction of a number of intrinsic properties, including constitutive properties and plasticity laws, as well as extrinsic factors, such as geometry and loading conditions. Standard techniques, such as the uniaxial tensile test, cannot provide all of the information relevant to predicting deformation and failure, especially for irradiated materials where low ductility limits the strain range that can be probed. Accordingly, we report progress in developing advanced methods to predict local deformation limits for fusion structures in terms of structural stress-strain [$\sigma(\varepsilon)$] or load-displacement (P-Δ) behavior, accounting for both intrinsic and extrinsic factors. The first step requires developing a self-consistent set of constitutive and plasticity laws for materials of interest, both unirradiated and irradiated.

In previous studies we developed self-consistent approach to derive $\sigma(\varepsilon)$ laws, that were successfully applied to 8-12Cr tempered martensitic steels and 14Cr oxide dispersion strengthened alloy irradiated in the Advanced Test Reactor (ATR). The approach is based on simultaneous measurements and finite element method (FEM) simulations of engineering stress-strain s(e) curves, which are consistent for a unique $\sigma(\varepsilon)$ law. Finding the unique $\sigma(\varepsilon)$ generally requires a few to many of iterations involving: (i) modifying input or previous iteration $\sigma(\varepsilon)$; (ii) re-running the FEM simulation; (iii) comparing simulated and experimental s(e) curves. In this report we use a MATLAB based code to automate the s(e) fitting.

Approach

The general approach is to measure P-Δ or engineering stress-strain [s(e)] curves and characterize and, in some cases, quantify large geometry changes (LGC) and deformation-flow (micro to macro) patterns of strain distributions (SD) for a wide variety of test geometries to access high stains and bound key structural conditions. Examples are shown in Figure1. The experimental information is combined with finite element modeling (FEM) of the corresponding specimen(s) during testing to simulate LGC behavior, P-Δ/s(e) and SD. The true-stress/strain constitutive equation $\sigma(\varepsilon)$ used in the finite element analysis is varied, and the computed values of P-Δ/s(e), LGC and SD compared to the measured values. Differences are used to adjust the $\sigma(\varepsilon)$, and the process proceeds iteratively to obtain a best fit maximum self-consistency.

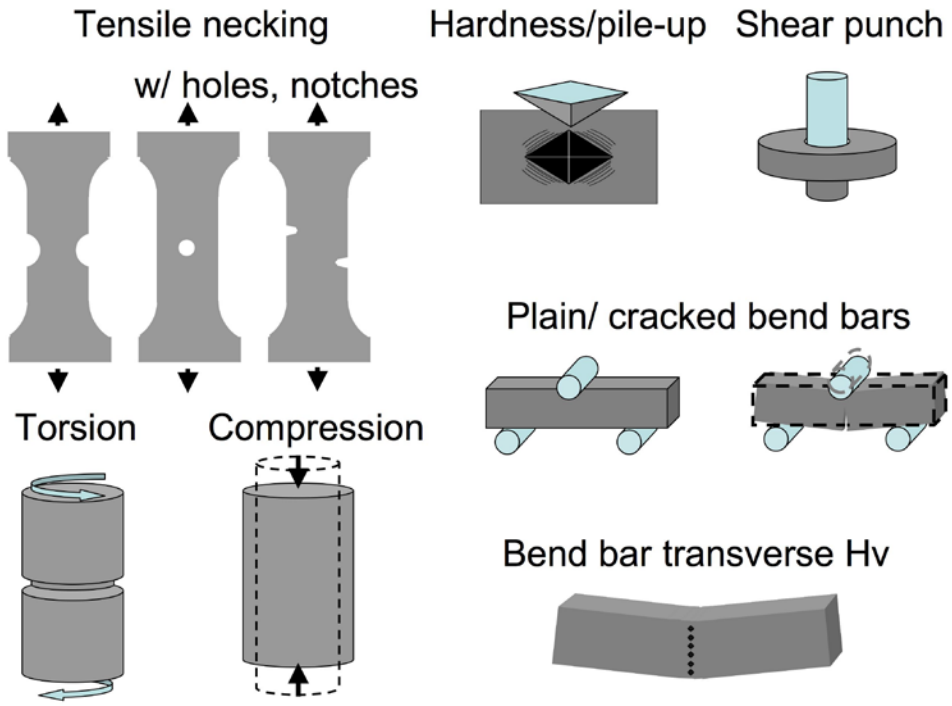

Figure 1. Examples of mechanical tests that can probe high strain behavior of structural materials coupled with FEM simulations to derive a self-consistent $\sigma(\varepsilon)$.

Automated Derivation of $\sigma(\varepsilon)$

Previous manual process consisted of the following components:

(i) Create an input $\sigma(\varepsilon)$ model, starting with the $s(e)_m$ converted to $\sigma(\varepsilon)$ up to the necking strain. The experimental $\sigma(\varepsilon)$ is then fit and extrapolated to higher strains by a 4 parameter dislocation theory based model that provides for strain hardening, softening and perfectly plastic behavior.

(ii) Use the current generation $\sigma(\varepsilon)$ as input to the FEM ABAQUS to predict the corresponding $s(e)_s$.

(iii) Parametrically adjust $\sigma(\varepsilon)$ based on a visual comparison the predicted and experimental $s(e)_m$ curves, iterating to self-consistent $s(e)_s \approx s(e)_m$ convergence.

In the semi-automated procedure, the iteration to find the best $\sigma(\varepsilon)$ model is controlled by a general MATLAB code "optGUI.m" which incorporates "optimizeFun.m" to manage an optimized fit. The workflow in the management code and its coupling to Excel and ABAQUS software is shown in Figure 2.Essential parameters are first defined in a graphical user interface (GUI) shown in Figure 3.

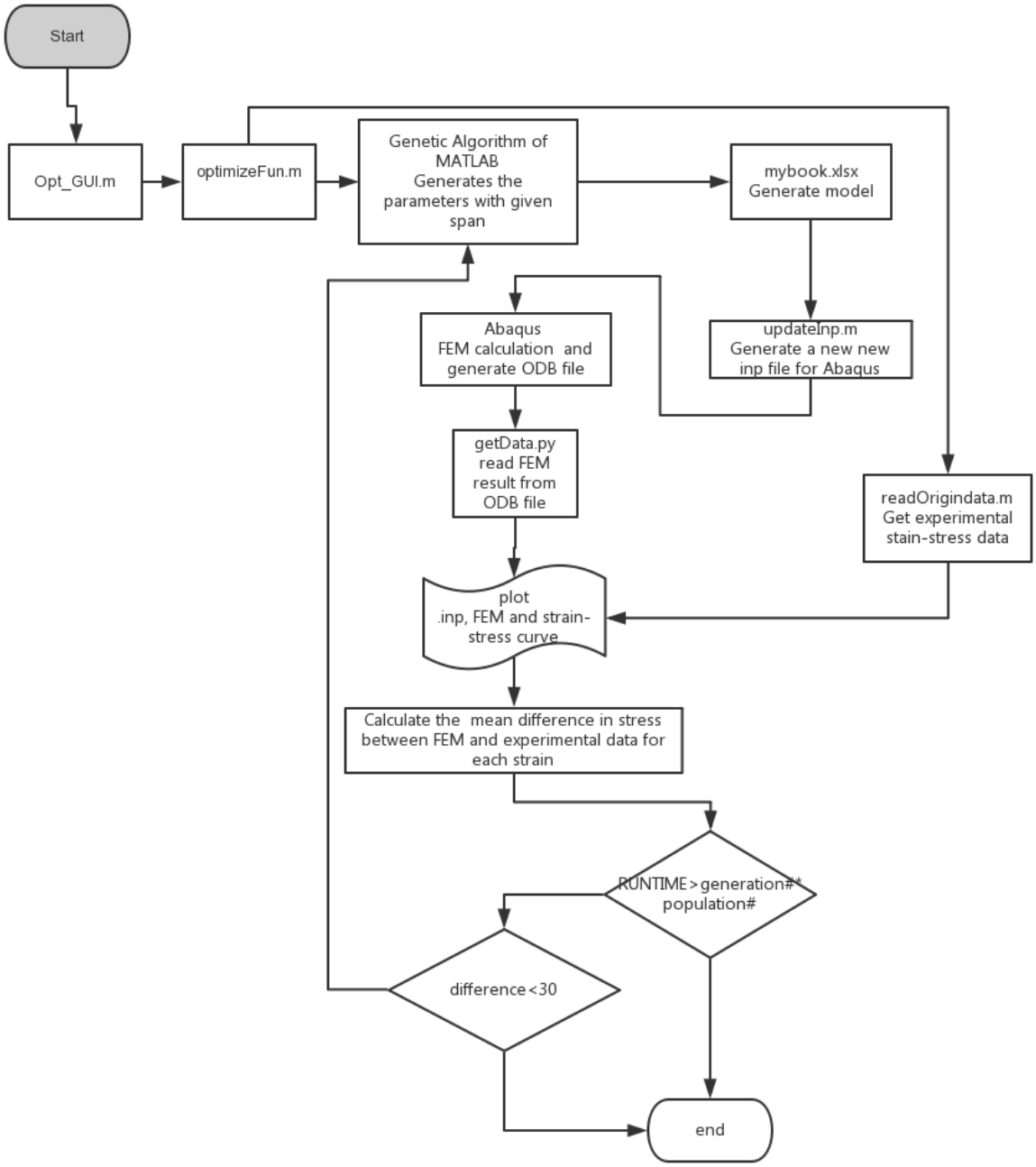

Figure 2. Schematic diagram of the optimization workflow.

1. In the optimizeFun.m MATLAB code, a *genetic* algorithm is used to randomly generate sets of $\sigma(\varepsilon)$ model parameters within a pre-defined space. The term *genetic* refers to a parameter optimization algorithm that mimics natural evolution process and is suitable for highly non-linear problems.

2. Each set of parameters are given to Excel spreadsheet "mybook.xlsx", that calculates the input $\sigma(\varepsilon)$ model in a form of true stress versus plastic strain table that is directly used as an input file for Abaqus.

3. After the Abaqus FEM simulation, the getData.py code reads the $s(e)_s$ results from the output database (ODB) file.

4. OptimizeFun.m plots experimental and FEM simulated engineering s(e) curves in one figure, and calculates the predicted versus measured s(e) difference for a specified set of strains.

5. Finally, optimizeFun.m best fits (optimizes) all the input parameters models with the genetic algorithm by repeating all the steps above until $s(e)_s \approx s(e)_m$.

The quality of the FEM results, in terms of a defined "Fitness" is shown in Eq. 1. As the sum of the square root of stress variances for each of the specified set of evaluation strains up to the onset of rapid stress decrease indicating the development of internal damage, the individual variances are weighted by a factor that decreases with increasing strain, indicting higher uncertainty and the possibility of internal damage prior to the rapid stress drop-off.

$$\text{fitness} = \sum_{e=0.01,0.02\ldots} \sqrt{\left\{\left|s_{FEM} - s_{Exp}\right|(1-\varepsilon)\right\}^2} \qquad (1)$$

Since the procedure is based on a general MATLAB algorithm that can deal with highly non-linear phenomena, which may have a number of local good fit minima, the algorithm is intended to mimic evolution by "natural selection". Fitness is the sum of the absolute predicted minus measured s(e) and is not a classical standard deviation. Indeed the fitness, with units of MPa, is much larger than the standard deviation. Initially, typically, 30 model parameter sets are selected randomly within a defined space. After each iteration, a subset of the models, including those that yield the best fit model are used to define a reduced parameter space, with a new selected set of 27 random model parameters added to the 3 best fit models. The average fitness is for all the models in one generation, while the best fitness is for the top 3 best models that are carried into the next generation. Thus the average model fit decreases with each generation due to the shrinking parameter space. The best fitness model average may also decrease, although typically to a much lesser extent. This so-called "natural selection" is intended to avoid the fitting becoming stuck in a local minimum.

Results

Figure 4 shows an example for the first individuals in the first generation s(e) curves for Eurofer 97 irradiated to 6.5 dpa in ATR at 295°C, that gives a relatively good initial fitness value of ≈ 437 since the parameter space was well known and narrowly defined in this case. The best and mean fitness values after 15 generations are 27 and 24MPa respectively in Figure 4(b) for ATR irradiated Eurofer97.However, such a good initial fitness is generally not observed. Figure 5 shows another example for a 14YWT alloy where the initial best and average fitness values are more than 300 and 1000 MPa, respectively. As the generations progress, the mean value decreases rapidly, as more low quality models are excluded in the shrinking parameter space. The single best parameter set is chosen as the final model when the Best fitness average falls below a specified value, like 200 MPa, in this example. The best and mean fitness values are 174 and 195 MPa respectively in Figure 5. Figure 6 shows the corresponding final optimized $s(e)_s$ and the $s(e)_m$ curves for the irradiated Eurofer 97 along with the control specimen. The classical standard deviation is 9.6 MPa for the irradiated condition and 12.7 MPa for the unirradiated control. Typically, optimization takes 60 iterations for unirradiated, and 150 iterations for irradiated conditions, respectively. Figures 7 and 8 summarize the corresponding results for the irradiated and the unirradiated conditions of F82H IEA with standard deviations of 3.2 and 3.4MPa, respectively, and for NF616 with corresponding standard deviations of 7.2 and 3.4 MPa. Figure 9 summarizes the corresponding results of 14YWT alloy in LT orientation tested at 800°C with standard deviations of 4.0 MPa,

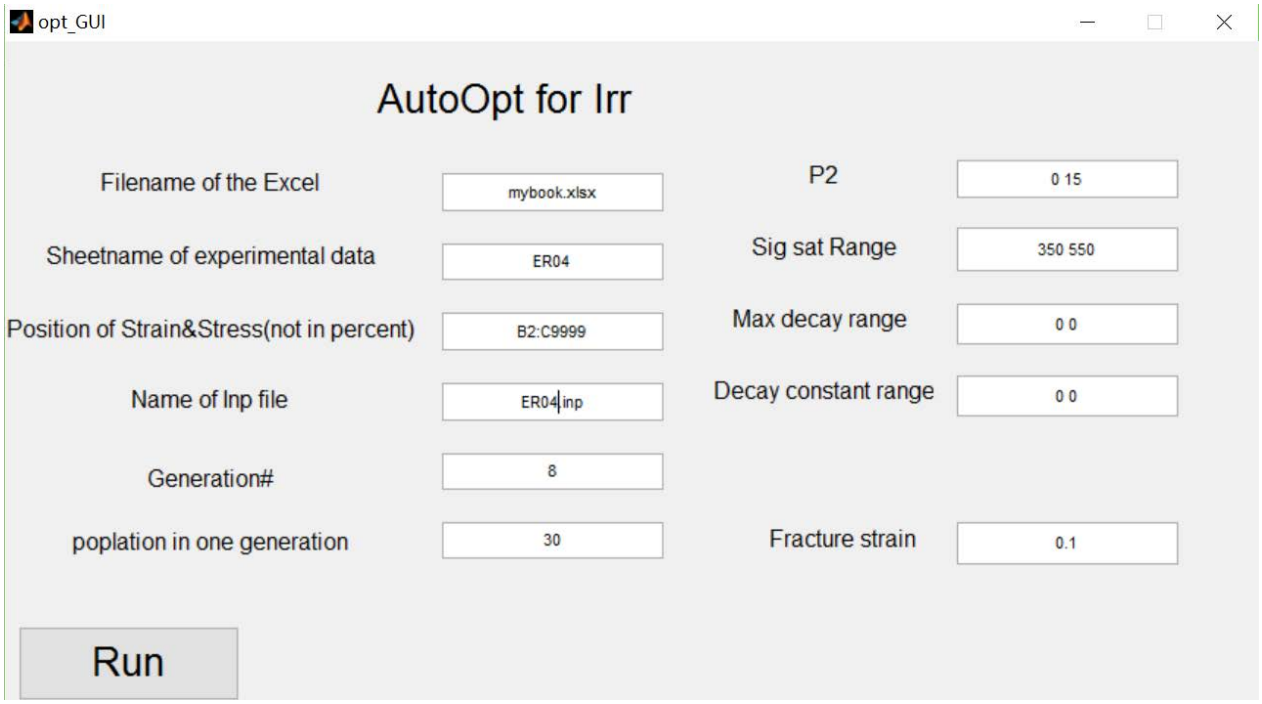

Figure 3. Graphical user interfaces to assign optimization data and iteration conditions

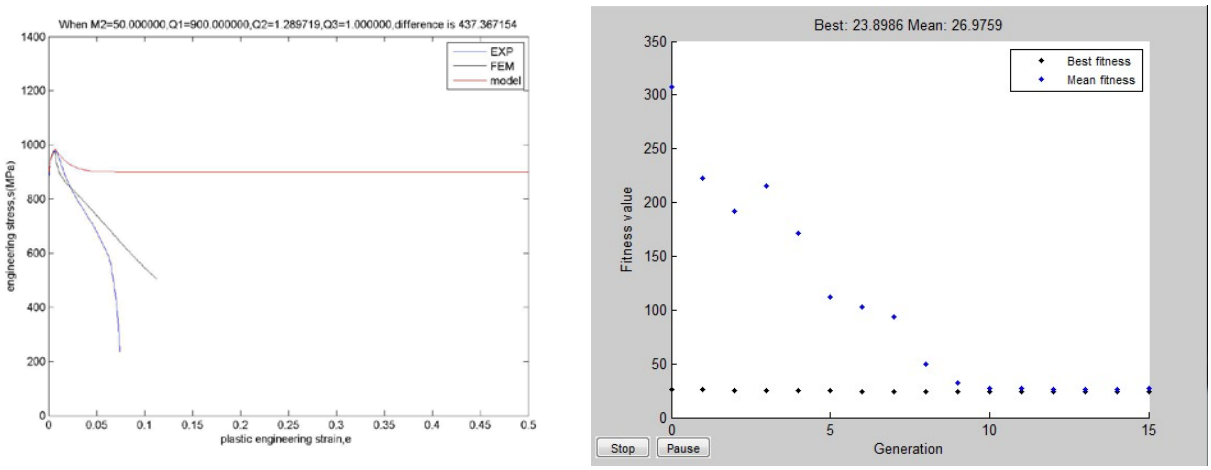

Figure 4. The first simulation in the first generation for ATR irradiated Eurofer 97(ER04).

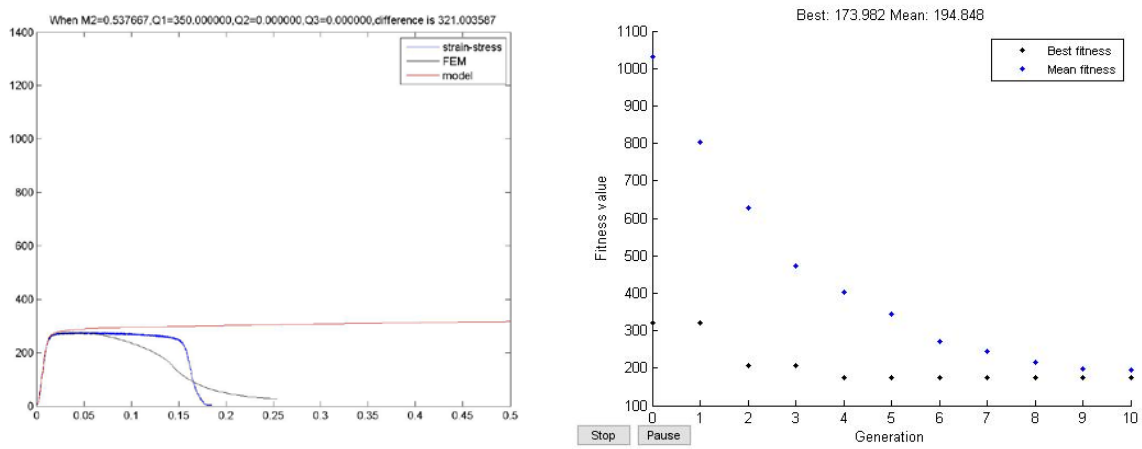

Figure 5. The first simulation in the first generation for 14YWT alloy (SSJ2_LT8_800c) and an example evolution of the mean and best fitness values as a function of generation.

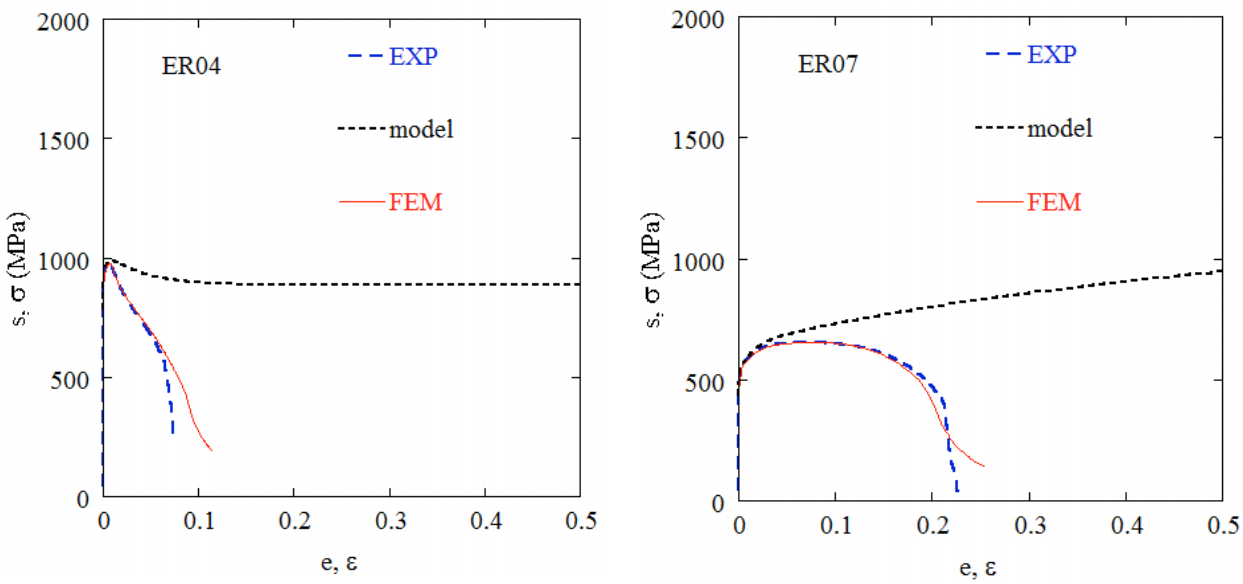

Figure 6. Comparison of experimental (EXP) and FEM simulated engineering s(e) curves along with the best optimized $\sigma(\varepsilon)$ model for (a) ATR irradiated Eurofer 97 (ER04) specimen and (b) the control specimen (ER07).

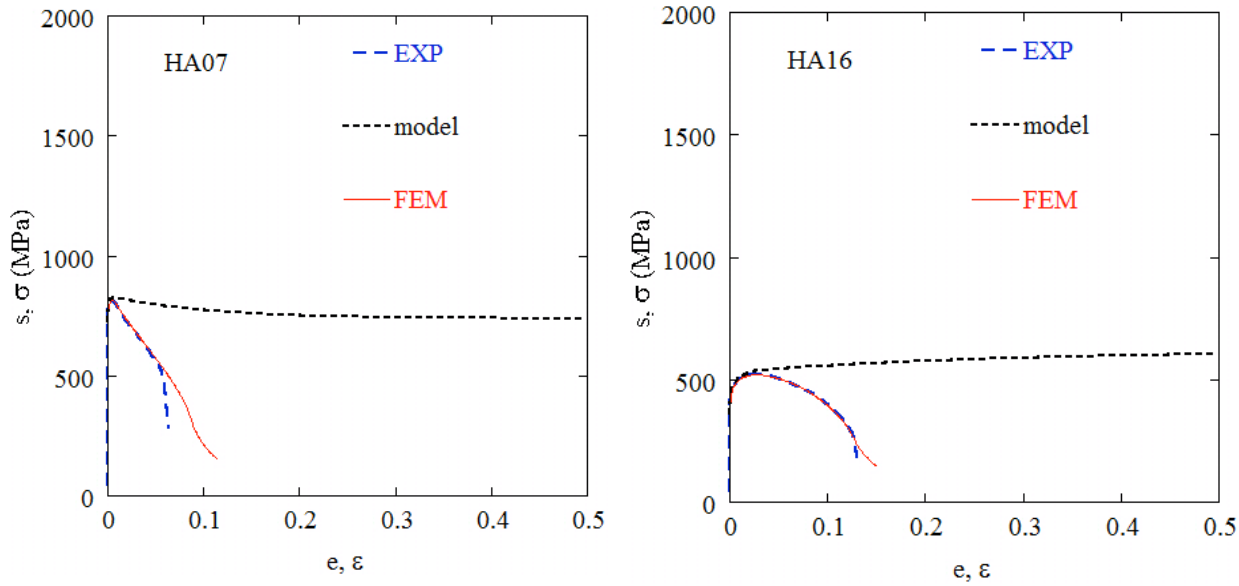

Figure 7. Comparison of experimental (EXP) and FEM simulated engineering s(e) curves along with the best optimized σ(ε) model for (a) ATR irradiated F82H IEA (HA07) specimen and (b) the control specimen (HA16).

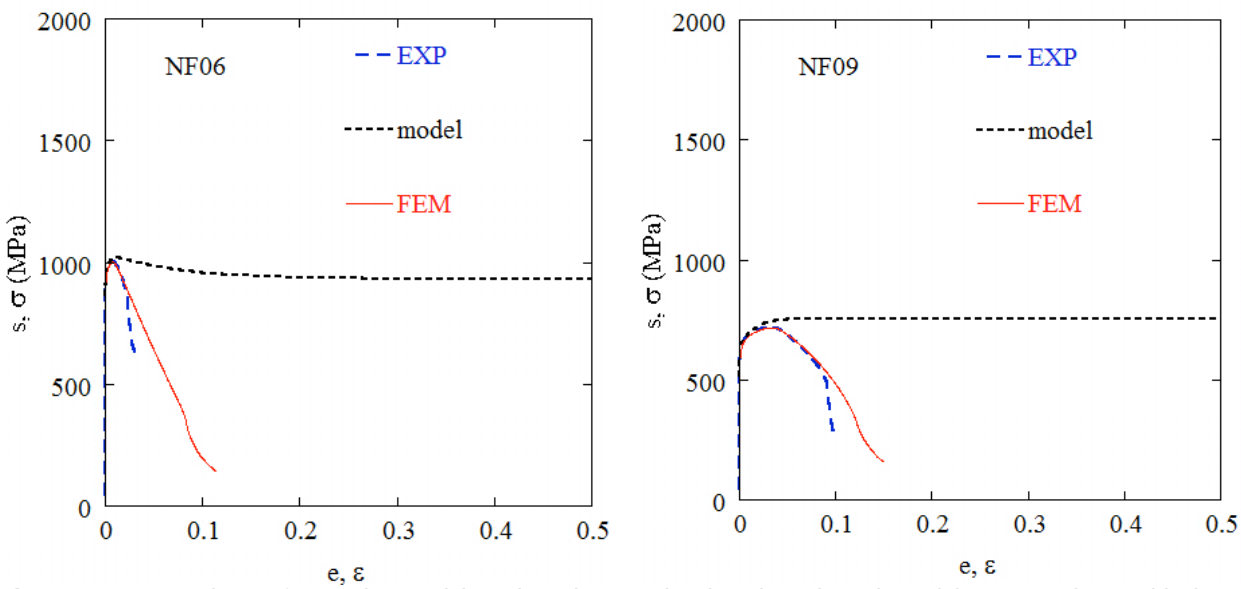

Figure 8. Comparison of experimental (EXP) and FEM simulated engineering s(e) curves along with the best optimized σ(ε) model for (a) ATR irradiated NF616 (NF06) specimen and (b) the control specimen (NF09).

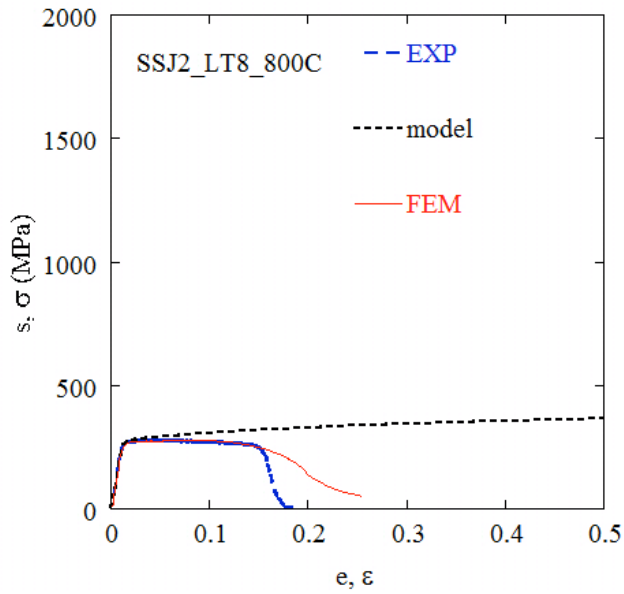

Figure 9. Comparison of experimental (EXP) and FEM simulated engineering s(e) curves along with the best optimized $\sigma(\varepsilon)$ model for a 14YWT alloy in LT orientation tested at 800°C.

Finally, we note that the difference between $s(e)_s$ and $s(e)_m$ at high strains in the rapid drop-off region is a measure of the development of load shedding internal damage. The opportunity to use this information to develop a better understanding of damage mechanics, including the effect of irradiation, will be exploited in the future.

Acknowledgements

The work at UCSB was funded by Office of Fusion Energy Science (DE-FG03-94ER54275) grants.

References:

[1.] T. Yamamoto, G.R. Odette, Y. Wu, Fusion Materials Semi-annual Report 7/1/2011 to 12/31/2011, DOE/ER-0311/51, (2012) 78-84.
[2.] T. Yamamoto, G.R. Odette, M.A. Sokolov, Journal of Nuclear Materials, 417 (2011) 115-119.
[3.] S.A. Maloy, T.A. Saleh, O.Anderoglu, T.J. Romero, G.R. Odette, T. Yamamoto, S. Li, J.I. Cole and R. Fielding, *J. Nucl. Mat.* 468 (2016) 232.
[4.] MathWorks, *Global Optimization Toolbox: User's Guide*(r2015b) http://in.mathworks.com/help/pdf_doc/optim/optim_tb.pdf.